ICES Journal of Marine Science, 62: 319–327 (2005)
doi:10.1016/j.icesjms.2004.07.031

Ecosystem indicators derived from satellite remotely sensed oceanographic data for the North Pacific

Jeffrey J. Polovina and Evan A. Howell

Polovina, J. J., and Howell, E. A. 2005. Ecosystem indicators derived from satellite remotely sensed oceanographic data for the North Pacific. – ICES Journal of Marine Science, 62: 319–327.

Satellite remotely sensed oceanographic data provide reliable global ocean coverage of sea surface temperature, sea surface height, surface winds, and ocean colour, with relatively high spatial and temporal resolution. We illustrate approaches to use these data to construct indicators that describe aspects of ecosystem dynamics in the North Pacific. Specifically, altimetry data are used to construct regional indicators of the ocean vertical structure, ocean colour data to describe the temporal chlorophyll dynamics of the coastal zone, ocean colour, sea surface temperature, and altimetry data to develop indices of biologically important ocean features, and finally altimetry data to drive a larval transport model and develop an index of larval retention. Recent changes in the North Pacific based on these indices are discussed.

Keywords: altimetry, ecosystem indicators, empirical orthogonal function, ocean colour, satellite oceanography, sea surface temperature.

Received 1 April 2004; accepted 27 July 2004.

J. J. Polovina and E. A. Howell: Ecosystem and Oceanography Division, Pacific Island Fisheries Science Center, NOAA Fisheries, 2570 Dole Street, Honolulu HI 96822-2396, USA. Correspondence to J. J. Polovina: tel: +1 808 983 5301; fax: +1 808 983 2901; e-mail: Jeffrey.Polovina@noaa.gov.

Introduction

Satellite sensors provide reliable global ocean coverage of sea surface temperature (SST), sea surface height (SSH), surface winds, and ocean colour, with high spatial and temporal resolution compared with *in situ* data. Most of these data are available at no cost to the user, and are available close to real time. Satellite-based oceanographic data have been used in a variety of ways in ecosystem research (Laurs and Polovina, 2000). For example, one common approach is to make maps covering short periods to identify oceanographic features such as fronts or eddies, and to evaluate the spatial pattern of higher trophic level animals relative to these features. However, as time-series of such data now exist that often are at least a decade long (and two decades in the case of SST), the data can be used to investigate temporal dynamics in the ocean that may have direct and indirect impacts on marine ecosystems. We illustrate how remotely sensed oceanographic data can be used to construct ecosystem indicators, with examples from the North Pacific focusing on regional ocean dynamics, ocean features, and larval transport.

Material and methods

Oceanographic parameters

The altimetry data used refer to a mapped global $0.3° \times 0.3°$ resolution product with a weekly resolution. The data are delivered as an anomaly created by subtracting the long-term average of the raw along-track profiles from 1993 to 1998. For the period between October 1992 and July 2002, data from the TOPEX/POSEIDON altimeter were used, and thereafter from JASON-1, which was put into operation along the same orbit and had a similar resolution. To compute the geostrophic currents, the 1994 NODC World Ocean Atlas Levitus long-term mean 1000-m dynamic height data set was added to the SSH anomaly files to create an "absolute" SSH. The east–west (x) and north–south (y) gradients, dz/dx and dz/dy, were derived from this height (z) and subsequently used to calculate the east–west (u) and north–south (v) components of the geostrophic current, as previously described (Polovina *et al.*, 1999).

SST data are derived from the five-channel Advanced Very High Resolution Radiometers (AVHRR) on board the

1054-3139/$30.00

NOAA-7, -9, -11 and -14 polar orbiting satellites. The data used from 1985 to July 2003 are from the descending (night-time) passes processed using versions 4.0 and 4.1 of the AVHRR Pathfinder SST algorithms developed by the University of Miami (Vazquez *et al.*, 1998). These data are received as a 9-km product mapped to an equal area projection for each week or month. From July 2003 to present, daily SST data processed using the NESDIS global area coverage (GAC) algorithm were averaged to create weekly and monthly images that are comparable on a temporal and spatial resolution to the Pathfinder SST product.

For ocean colour purposes, chlorophyll *a* pigment concentrations were taken from three sensors. Data for the period 1979−1986 were derived from the Coastal Zone Color Scanner (CZCS) on board the Nimbus-7 satellite. These data were delivered as an 18-km pixel-resolution product mapped to an equal area projection. The most recent reprocessing by the Laboratoire de Physique et Chimie Marines (Antoine *et al.*, 2003) was used, providing a data set spanning the periods 1978−1983 and 1985−1986. Data for 1984 were not present in the reprocessed data set because of insufficient coverage. For 1997, chlorophyll *a* data collected by the Ocean Color and Temperature Scanner (OCTS) on the ADEOS satellite were used. These data (version 4) were delivered as a 9-km pixel resolution product mapped to an equal area projection. From September 1997 to present, chlorophyll *a* data collected by the Sea-viewing Wide Field-of-view Sensor (SeaWiFS) instrument on board the Seastar spacecraft were used. This product is derived from the raw measured wavelength bands using the SeaWiFS algorithm (SeaWiFS L3 CHLO product), and distributed as version 4. These data are a 9-km pixel-resolution product on an equidistant cylindrical projection.

Empirical orthogonal function analysis

Remotely sensed oceanographic data sets are often relatively large, and provide a challenge to distil into indices that capture significant spatial and temporal dynamics. One method is to use principal components analysis, more commonly known in ocean sciences as empirical orthogonal function analysis (EOF; Emery and Thomson, 2001).

To prepare the altimetry data for EOF analysis, the monthly SSH product was resampled to a lower spatial resolution. A median filter with a 1° smoothing window length was used, maintaining the same approximate number of sample points across different sized areas of analysis (1° × 1° area for the Alaskan Gyre, and the eastern Pacific; 2° × 0.5° for the central North Pacific; and 2° × 1° for the equatorial area of interest). This time-series of monthly SSH was detrended and standardized by removing the monthly periodic signal and subtracting the long-term mean. Land values were removed to create the final, detrended matrix F(x,t), which was then decomposed using the form

$$F(x,t) = \sum_{i=1}^{N} a(t)\phi_i(x)$$

where $a_i(t)$ are the principal components (temporal expansion coefficients) of the spatial components $\phi_i(x)$ (Wilson and Adamec, 2001). The temporal and spatial components are calculated from the eigenvectors and eigenfunctions of the covariance matrix R, where $R = F' * F$. This analysis results in N statistical modes, each with a vector of expansion coefficients related to the original data time-series by

$$a_i = F\phi_i$$

and a corresponding spatial component map ϕ_i. Each of these maps represents a standing oscillation, and the expansion coefficients represent how this pattern oscillates through time. Each of these modes are orthogonal and by definition uncorrelated with respect to each other, with the variance calculated by

$$\sigma_i^2 = \frac{\lambda_i}{\sum_{i=1}^{N} \lambda_i}$$

where λ_i is the eigenvalue for each mode (i = 1…N).

One hundred kilometre coastline extraction

A 100-km data extraction mask was created to evaluate only those data lying within 100 km of the eastern Pacific continental boundary. To minimize the number of curves in the coastline, the mask was initialized using the GMT pscoast command for low-resolution data, followed by interpolation and reduction using the MATLAB interpm and reducem functions. This resulted in a continuous, relatively smooth, coastline from 23°N to 62°N, covering the western United States, Canada, and Alaska. All data within 100 km of this coastline were then extracted from SeaWiFS, using the GMT gmtselect and grdmask commands to create the final extraction mask.

Results and discussion

Regional indicators

Time-series of the EOFs derived from SSH estimated with satellite altimetry provide indicators that describe temporal and spatial changes in geostrophic transport and the ocean's vertical structure, especially changes in the depth of the top of the thermocline, which may have important ecosystem implications. In the equatorial region, Rebert *et al.* (1985) estimated that for each 1-cm change in SSH, the depth of the top of the thermocline changes by 200 cm in the opposite direction. This approach is illustrated with four regional EOFs (Figures 1a−d). In the equatorial regions,

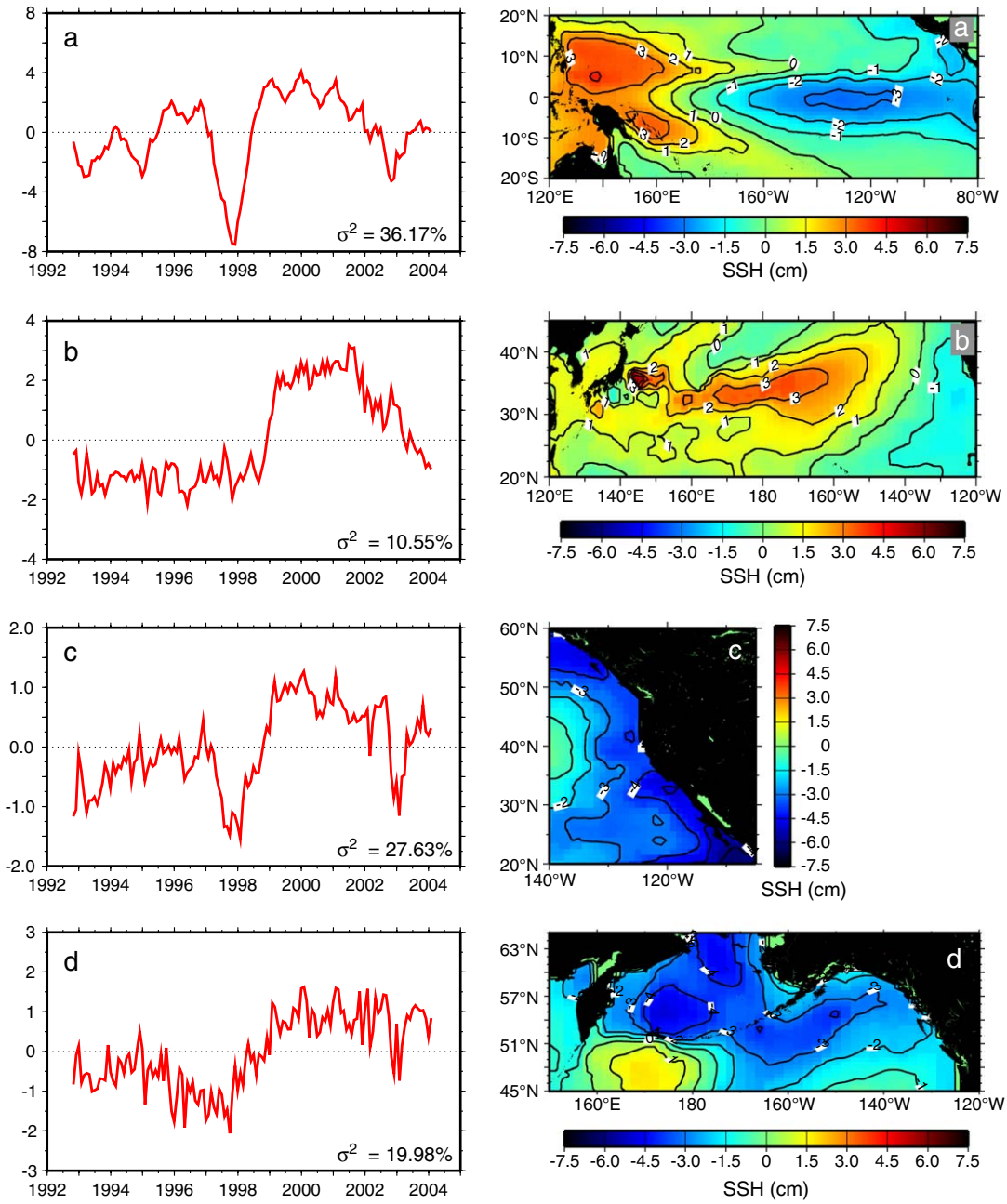

Figure 1. The first EOF modes of SSH for (a) the equatorial Pacific, (b) the central North Pacific, (c) the eastern Pacific, and (d) the Alaskan Gyre. Left panels, weighting functions expressed as time-series (with annotation of the variance explained); right panels, corresponding spatial patterns.

the first EOF captures 36% of the monthly SSH variation, with a spatial pattern where the eastern and western Pacific vary in an opposite manner (Figure 1a). During the strong 1997−1998 *El Niño*, the SSH in the western Pacific dropped by as much as 28 cm, whereas that in the eastern North Pacific rose by 28 cm. This indicator shows that the 2002−2003 *El Niño* had a much weaker impact on equatorial SSH than the 1997−1998 event. Also beginning in 1999, there was a 3-year response in SSH characterized by a drop in the eastern Pacific and a rise in the western Pacific, possibly a response from the 1999 *La Niña*. This SSH EOF may be basically an *El Niño* indicator but, because it is based on SSH rather than SST or atmospheric pressure, it better describes changes in vertical

structure and geostrophic transport than the more traditional indices.

The next regional indicator is the first SSH EOF from the mid-latitude region, defined as 20−45°N, and it captures 11% of the monthly variation. This indicator identifies an abrupt change in SSH in 1999, characterized by SSH rising in the central North Pacific (Figure 1b). This increase represents an increase in heat content, stratification, and depth of the top of the thermocline. The change persisted for several years, but by 2004, conditions returned to baseline levels, suggesting a response to the strong 1999 *La Niña*.

The third regional indicator is the first SSH EOF from the eastern North Pacific (20−60°N), and it explains 33% of the monthly variation. This indicator shows a sharp and more persistent drop in 1999, interrupted by the relatively strong mid-latitude 2002−2003 *El Niño* (Figure 1c). The drop in SSH indicates an elevation of the top of the thermocline.

The fourth regional indicator is the first SSH EOF for the Gulf of Alaska and Bering Sea, north of 45°N, and explains 20% of the monthly variation. This indicator shows a drop in SSH, which developed more gradually than in the eastern North Pacific, beginning in 1999 and persisting through 2004, with minimal impact from the 2002 to 2003 *El Niño* (Figure 1d).

Summarizing, these four regional EOFs distil more than a decade of SSH data in the North Pacific to identify some major spatial and temporal patterns of ocean dynamics. From the perspective of impacts on the vertical structure, the 1997−1998 *El Niño* was very strong in the equatorial region, but relatively weak at higher latitudes, whereas the 2002−2003 *El Niño* had the opposite impact. Also beginning in 1999, the change observed in vertical structure was relatively weak in the equatorial regions (an increase in SSH persisting for only 3 years), but strong in higher latitudes (a drop in SSH persisting through the present).

Satellite-derived surface chlorophyll data can also be used to construct regional indicators. Given that the highest levels of surface chlorophyll are located in a band along the perimeter of the North Pacific, from the shore to several hundreds of kilometres offshore, we examined chlorophyll dynamics in this region, because it may be a useful indicator to describe surface phytoplankton dynamics. Typically, surface chlorophyll data are extracted in rectangular boxes defined by longitude and latitude.

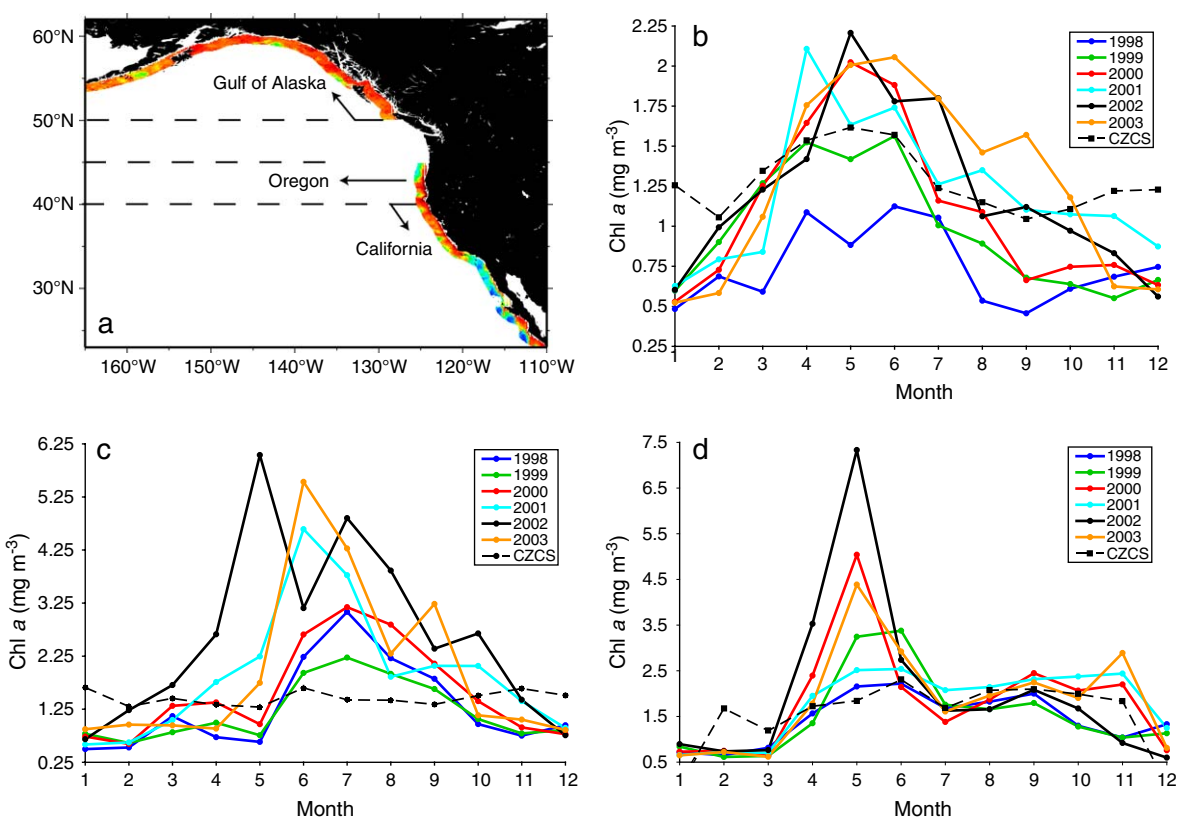

Figure 2. Average values of surface chlorophyll *a* in a band spanning from the coastline to 100 km offshore, for (a) the entire coastal area, and monthly means by year (SeaWiFS data) or period (CZCS data) for (b) California (23−40°N), (c) south Oregon (40−45°N), and (d) Gulf of Alaska (50−62°N).

However, our approach allowed us to extract surface chlorophyll from a band from nearshore to 100 km offshore along the eastern and northeastern North Pacific (Figure 2a). A time-series of monthly means from this coastal band averaged along sections of coastline provides indices of surface phytoplankton biomass. For illustration, three coastal regions are selected: California, southern Oregon, and the Gulf of Alaska (Figure 2b–d). SeaWiFS data provided monthly averages by year, and CZCS were combined over the life of the sensor because of limited coverage. All three time-series show significant seasonal variation and different interannual patterns.

Although these time-series are relatively short, chlorophyll levels were highest after 1999 in all regions. In California, SeaWiFS values generally are consistent with the CZCS mean (although the seasonal trend differs), whereas in Oregon and Alaska, recent values are considerably higher in spring, suggesting increases in coastal ocean productivity there. Such data might be used to construct an index of the productivity of fish habitat along the coast.

Indicators of features

Boundaries between ecological regions or provinces are one feature that can be identified and monitored with satellite data. This concept will be illustrated with an example from the central North Pacific. Satellite imagery of surface chlorophyll in the North Pacific shows a persistent region of relatively low surface concentration representing the subtropical gyre, and to the north a region of high surface concentration representing the Transition Zone and Subarctic gyre. The boundary between these two provinces, defined by a chlorophyll front (well-contoured and indicated by the 0.2 mg m^{-3} surface concentration), has been termed the Transition Zone Chlorophyll Front (TZCF), and is an important migration and forage habitat for large pelagic species (Polovina *et al.*, 2001). Using SeaWiFS ocean colour satellite imagery, the TZCF can be easily plotted (Figure 3a). The position of the TZCF migrates north and south seasonally by about 1000 km. In summer, as the central North Pacific warms and becomes more stratified, the TZCF typically shifts north to 40–45°N,

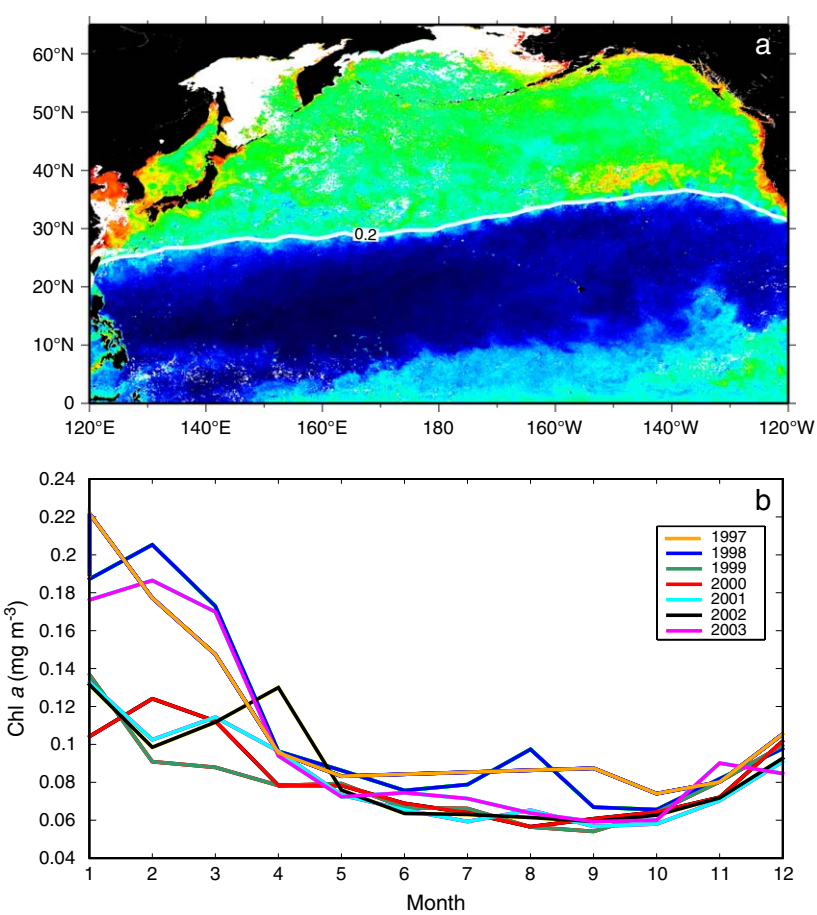

Figure 3. (a) SeaWiFS ocean colour for February 2000 (white line: 0.2 mg m^{-3} Transition Zone Chlorophyll Front, TZCF), and (b) monthly chlorophyll *a* values, 1997–2003, in a box (179.5°E–174.5°W, 28–30°N) around Midway and Kure Atolls.

whereas in winter, as storm tracks shift south and vertically mix the central North Pacific, the TZCF moves south to about 28–32°N (Polovina *et al.*, 2001). However, the winter position of the TZCF varies considerably. In some years, it reaches sufficiently far south to impinge on the northern atolls of the northwestern Hawaiian Islands; in others its winter position lies hundreds of kilometres to the north. Monthly time-series of surface chlorophyll for the region around the northern atolls reveal high values in 1997, 1998, and 2003, caused by a southward shift of the TZCF (Figure 3b). In winters when the TZCF impinges on the northern atolls, the habitat is characterized by higher chlorophyll, vertically mixed cooler water, and a convergent front that appears to support a variety of large pelagic species, including squid, tuna, and turtles (Polovina *et al.*, 2001, 2004). However, in winters when the TZCF is well north of the atolls, the habitat consists of strongly vertically stratified, low chlorophyll, warm water, and no productive front (Polovina *et al.*, 2001). The winter position of the TZCF provides one measure of the northern boundary of the subtropical gyre. Tracking this front over time provides an indicator of the dynamics of a basin-scale feature, and large-scale atmospheric and ocean changes.

Eddies can also be observed and monitored by satellites, and indicators can be derived from SST data for a cyclonic (cold core) eddy off Kona coast of the Big Island of Hawaii, and from SSH for the anticyclonic (warm core) Sitka eddy in the Gulf of Alaska. The cyclonic eddies developing off the Kona coast are very visible from the cold subsurface water that is pumped to the surface at their centre, and research cruises have documented their significant impact on lower trophic levels at these locations (Seki *et al.*, 2001). The Sitka eddy is a mesoscale feature with rotational speeds as high as 50 cm s^{-1} that develops off southeast Alaska roughly every other year (Healey *et al.*, 2000). The presence of the Sitka eddy affects the flow of the Alaska

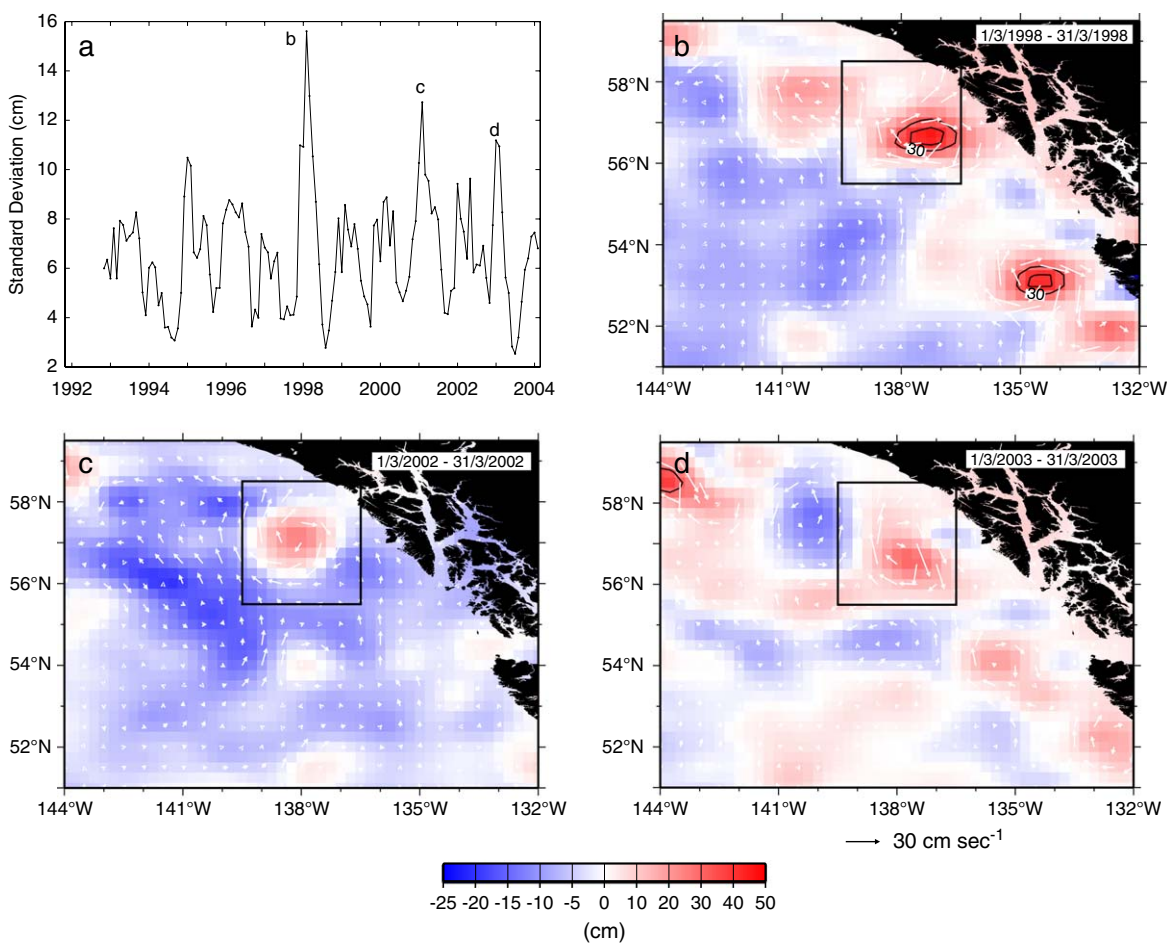

Figure 4. (a) Time-series of the monthly standard deviation of TOPEX/POSEIDON and JASON-1 SSH in the Sitka region of the Gulf of Alaska (identified by the box in panels b, c, and d), 1992–2004, and corresponding spatial patterns of SSH for three months (identified in panel a) with high standard deviations, in (b) March 1998, (c) March 2002, and (d) March 2003 (geostrophic currents derived from altimetry data are represented by the white vectors in panels b–d).

Current, so having an impact on salmon and other species in the region. The anticyclonic Sitka eddy is most detectable by the elevated SSH at its core.

For the two regions, time-series of the standard deviation of the mean monthly SST and SSH, indicate the presence of an eddy when values are high. This is because an eddy perturbs the relatively homogenous spatial SST/SSH fields, resulting in high standard deviations. For example, high SSH standard deviation in March 1998, March 2002, and March 2003 identify the Sitka eddy (Figure 4). High SST standard deviation in August 1999, October 2000, and November 2002 identify the Kona eddies (Figure 5).

Indicators derived from models

Within the physical oceanographic community, satellite data such as SSH and SST are assimilated into circulation models, whereas those such as wind are used to drive their models. Biologists may want to use the information for biological models. For example, estimates of surface chlorophyll might be used to either tune or drive ecosystem models. Models of spatial movement of large pelagic species might be driven by data that define preferred habitat. We here illustrate such use of satellite data to drive a model of larval transport, and derive an index of larval retention for an atoll in the Hawaiian archipelago. Geostrophic currents, caused largely by eddies, appear to be an important factor in larval transport. Polovina *et al.* (1999) simulated transport of spiny lobster larvae released from various islands and banks in the archipelago with geostrophic current vectors estimated from 10-day TOPEX/POSEIDON satellite altimetry. Local deepwater snapper species have a three-month larval period. Using the same model, we developed an index of deepwater snapper larval retention by simulating a monthly release of larvae from Midway Atoll, and computing the fraction retained within 140 km of the atoll three months later. This index shows considerable temporal variation caused by the variation in geostrophic currents (Figure 6), indicating periods of low

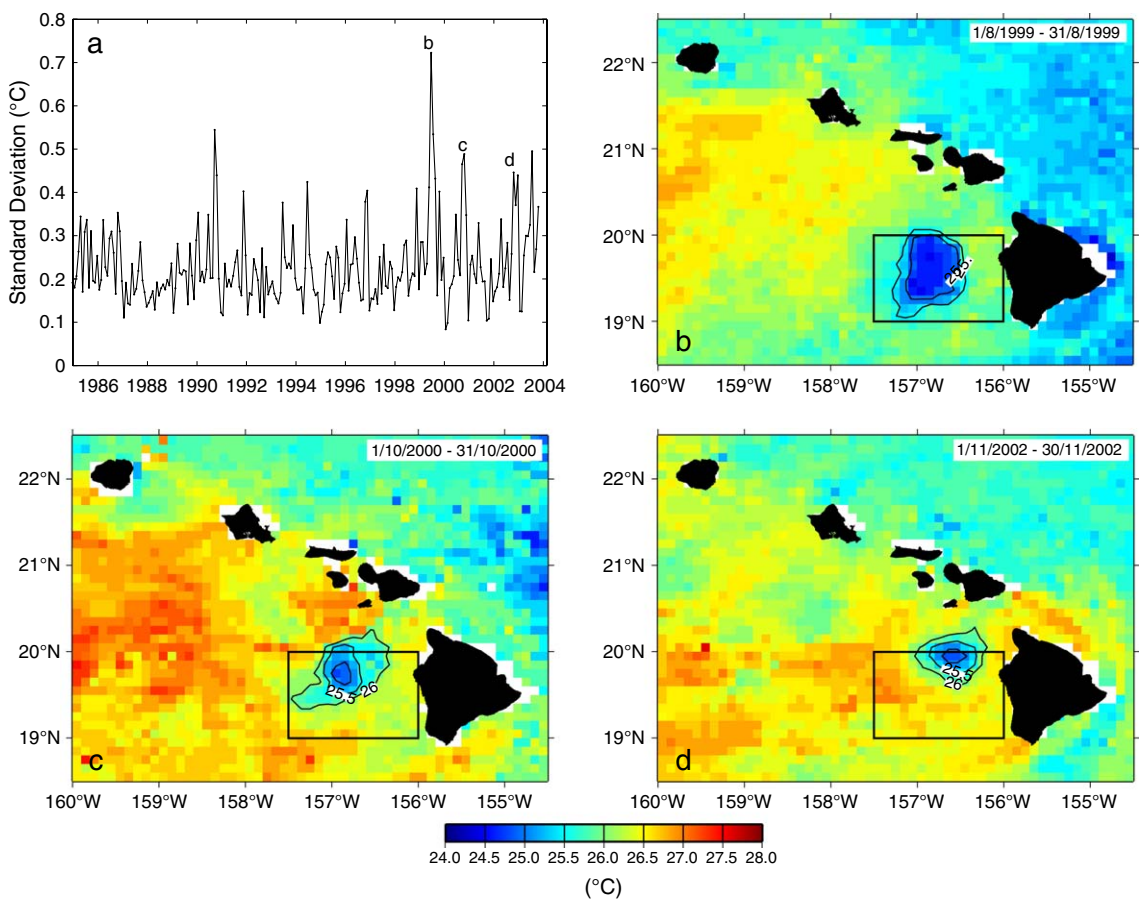

Figure 5. (a) Time-series of monthly standard deviation of AVHRR Pathfinder SST in a region off the Kona coast of Hawaii (identified by the box in panels b, c, and d), 1985–2003, and corresponding spatial patterns of SST for three months (identified in panel a) with high standard deviations, in (b) August 1999, (c) October 2000, and (d) November 2002.

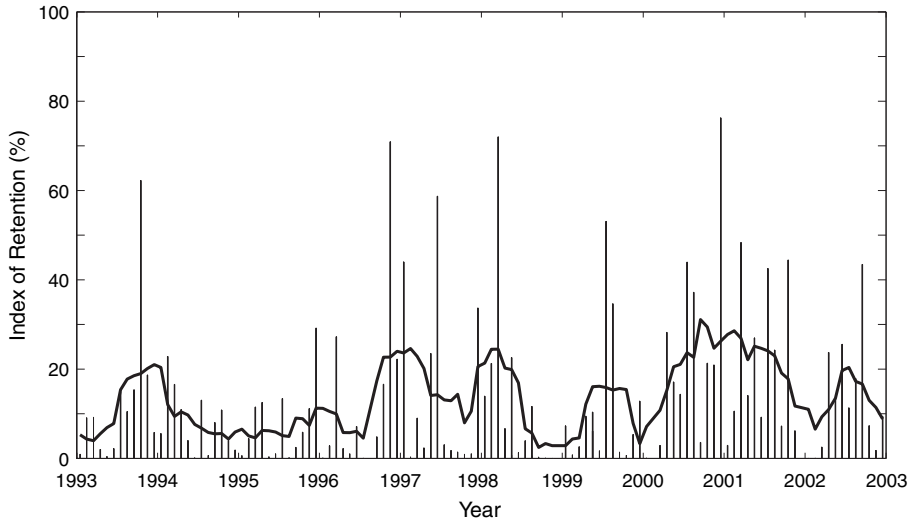

Figure 6. Time-series of the percentage of simulated larvae retained within 140 km of the Midway Atoll, three months after release, 1993−2003 (the line represents the six-month moving average).

retention in 1995 and 1996, and periods of high retention in 2000 and 2001 (Figure 6). This model could be expanded to describe larval growth as a function of satellite-derived estimates of SST encountered by the larvae, and surface or Ekman transport impacts on diurnally migrating larvae estimated from satellite-derived windfields.

Summarizing, remotely sensed oceanographic data provide global data almost in real time, covering surface winds, surface temperature, surface chlorophyll, and sea surface height. Although these data alone do not fully describe ecosystem dynamics, they can make an important contribution to a suite of indicators, reflecting regional differences, specific features, and model-derived properties.

Acknowledgements

We thank Donald Kobayashi for his help in preparing the larval retention index and for reviewing an early draft of this manuscript. CZCS ocean colour data were produced by the Laboratoire de Physique et Chimie Marines, and obtained from the Rosenstiel School of Marine and Atmospheric Sciences remote sensing laboratory. OCTS data used were produced by the National Space Development Agency of Japan. The SeaWiFS ocean colour data used were produced at the Goddard Space Flight Center. These two products were obtained from the Goddard Distributed Active Archive Center (DAAC), under the auspices of the National Aeronautics and Space Agency. Altimetry data used were produced by the Ssalto program and obtained from Collecte Localisation Satellites (CLS), under the auspices of the Centre National d'Études Spatiales of France. SST data were produced by the Pathfinder project at the Jet Propulsion Laboratory. These data were obtained from the Physical Oceanography Distributed Active Archive Center, under the auspices of the National Aeronautics and Space Agency.

References

Antoine, D., Morel, A., Gentili, B., Gordon, H. R., Banzon, V., Evans, R. H., Brown, J. W., Walsh, S., Baringer, W., and Li, A. 2003. In search of long-term trends in ocean color. EOS Transactions of the American Geophysical Union, 84(301): 308−309.

Emery, W. J., and Thomson, R. E. 2001. Empirical orthogonal functions. *In* Data Analysis Methods in Physical Oceanography, pp. 319−343. Elsevier Science, Amsterdam.

Healey, M. C., Thomson, K. A., Leblond, P. H., Huato, L., Hinch, S. C., and Walters, C. J. 2000. Computer simulations of the effects of the Sitka eddy on the migration of sockeye salmon returning to British Columbia. Fisheries Oceanography, 9: 271−281.

Laurs, R. M., and Polovina, J. J. 2000. Satellite remote sensing: an important tool in fisheries oceanography. *In* Fish and Aquatic Resources Series 4. Fisheries Oceanography: An Integrative Approach to Fisheries Ecology and Management, pp. 146−157. Ed. by P. J. Harrison, and T. R. Parsons. Blackwell Science, Oxford. 347 pp.

Polovina, J. J., Balazs, G. H., Howell, E. A., Parker, D. M., Seki, M. P., and Dutton, P. H. 2004. Forage and migration habitat of loggerhead (*Caretta caretta*) and olive ridley (*Lepidochelys olivacea*) sea turtles in the central North Pacific Ocean. Fisheries Oceanography, 13: 36−51.

Polovina, J. J., Howell, E., Kobayashi, D. R., and Seki, M. P. 2001. The Transition Zone chlorophyll front, a dynamic global feature defining migration and forage habitat for marine resources. Progress in Oceanography, 49: 469−483.

Polovina, J. J., Kleiber, P., and Kobayashi, D. 1999. Application of TOPEX/POSEIDON satellite altimetry to simulate transport dynamics of larvae of the spiny lobster (*Panulirus marginatus*), in the northwestern Hawaiian Islands, 1993−96. Fishery Bulletin US, 97: 132−143.

Rebert, J. P., Donguy, J. R., Eldin, G., and Wyrtki, K. 1985. Relations between sea level, thermocline depth, heat content, and dynamic height in the tropical Pacific Ocean. Journal of Geophysical Research, 90(C6): 11719–11725.

Seki, M. P., Polovina, J. J., Brainard, R. E., Bidigare, R. R., Leonard, C. L., and Foley, D. G. 2001. Biological enhancement at cyclonic eddies tracked with GOES thermal imagery in Hawaiian waters. Geophysical Research Letters, 28: 1583–1586.

Vazquez, J., Perry, K., and Kilpatrick, K. 1998. NOAA/NASA AVHRR Oceans Pathfinder Sea Surface Temperature Data Set User's Reference Manual Version 4.0, JPL Publication D-14070.

Wilson, C., and Adamec, D. 2001. Correlations between surface Chlorophyll and sea surface height in the tropical pacific during the 1997–1999 El Niño-Southern Oscillation event. Journal of Geophysical Research, 106: 31175–31188.